Exp Fluids (2014) 55:1735
DOI 10.1007/s00348-014-1735-3

RESEARCH ARTICLE

Evaluation of hot-wire spatial filtering corrections for wall turbulence and correction for end-conduction effects

M. A. Miller · B. Estejab · S. C. C. Bailey

Received: 30 September 2013 / Revised: 28 March 2014 / Accepted: 17 April 2014 / Published online: 6 May 2014

Abstract Several recent spatial filtering corrections for Reynolds stress measured by single component hot-wire probes were assessed using turbulent channel flow data measured over a moderate Reynolds number range. Using measurements with a variety of hot-wire lengths and aspect ratios, the current work determines the impact of these corrections on the actual magnitude and Reynolds number dependence of the near-wall turbulent peak in Reynolds stress and compares it to results from prior direct numerical simulations of turbulent channel flow. Comparison of the results following application of previously published correction schemes were found to produce similar results, with some limitations observed for each technique. Comparison to direct numerical simulation results suggested that additional corrections were needed to correct for end conduction effects. An additional modification for these effects was devised which improved agreement between probes of different lengths and aspect ratios and improved agreement between the measured and direct numerical simulation results.

Present Address:
M. A. Miller
Department of Mechanical and Aerospace Engineering, Princeton University, Princeton, NJ, USA

Present Address:
B. Estejab
Department of Mechanical Engineering, Virgina Tech, Blacksburg, VA, USA

S. C. C. Bailey (✉)
Department of Mechanical Engineering, University of Kentucky, Lexington, KY, USA
e-mail: sean.bailey@uky.edu

1 Introduction

Considerable effort has been undertaken to understand the mean flow and Reynolds stress scaling of wall-bounded flows. This has led to numerous experimental facilities being developed specifically to reach high Reynolds number conditions. However, with the addition of these new facilities, the instrumentation employed has to provide with much higher spatial resolution, and frequency response, in order to accurately capture the smallest scales of turbulence. At high Reynolds numbers, hot-wire anemometers continue to be used in the study of turbulence, due to their frequency response characteristics.

As noted in Smits et al. (2011), a definition of high Reynolds number wall-bounded flow is one where the friction Reynolds number, $Re_\tau = hu_\tau/\nu$, where u_τ is the friction velocity, ν the kinematic viscosity, and h the thickness of the wall layer, must be large enough so that a well-defined log region of overlap forms between the largest and smallest scales of turbulent eddies. A variety of ranges have been cited as being required to achieve these high Re_τ conditions; ranging from $Re_\tau \approx 5{,}000$ (Smits et al. 2011) to $Re_\tau \approx 20{,}000$ (Hultmark et al. 2012). For a fixed h, this also requires that the sensor size must be reduced to fully capture the eddies which scale on the order of the Kolmogorov length scale, $1.5 - 2.0\,\nu/u_\tau$ near the wall (Ligrani and Bradshaw 1987; Yakhot et al. 2010). If these eddies are not fully resolved, the measured Reynolds stresses are significantly lower than the true Reynolds stress. As an example, to fully resolve these scales in a facility with h of $\mathcal{O}(0.1)$ m at $Re_\tau = 5{,}000$ a hot-wire must be $\mathcal{O}(20)$ μm in length to fully resolve the smallest eddies, which is not possible using most current methods of constructing hot-wires without significant end-conduction error. Ligrani and Bradshaw (1987) was the first complete

investigation into the effects of the ratio of length, l, to diameter, d, as well as the viscous wire length, $l^+ = lu_\tau/\nu$ on the spatial resolution and end conduction of hot-wires in wall-bounded turbulence. Their originally proposed recommendations to keep $l/d > 200$ and $l^+ < 20$ have remained largely intact despite more recent investigations (for example see Hultmark et al. 2011; Hutchins et al. 2009; Li et al. 2004).

Limitations imposed by the geometry specifications required to avoid hot-wire spatial filtering and end conduction effects have introduced difficulties in the measurement of turbulence in high Re_τ facilities. More recent developments to address these limitations have included new methods of creating nano-scale hot-wires using MEMS techniques (Bailey et al. 2010; Vallikivi et al. 2011), which alleviates this problem. However, at the very high values of Re_τ which can be achieved in specialized facilities, even these probes can be susceptible to spatial filtering effects and require additional corrections (Hultmark et al. 2012, 2013).

To allow examination of the streamwise Reynolds stress, $\overline{u^2}$, scaling in high Re_τ flows, several correction schemes have been recently proposed to counter the effects of spatial filtering in the anisotropic turbulence of wall-bounded flows (Chin et al. 2009, 2011; Hutchins et al. 2009; Monkewitz et al. 2010; Philip et al. 2013b; Segalini et al. 2011; Smits et al. 2011).

These schemes vary significantly in their theoretical or empirical bases but have largely been validated via filtered DNS, or by comparing the collapse of corrected profiles at different l^+ using only the Hutchins et al. (2009) [and sometimes the Ng et al. (2011)] data sets. Despite this proliferation of correction schemes, very little comparison between results corrected by the different schemes has been performed. The exception being Segalini et al. (2011), who compared their corrected results to those found using the Monkewitz et al. (2010) and Marusic et al. (2010) [an early form of the Smits et al. (2011) correction] at a single Reynolds number. Here, we provide a comparison and evaluation of several of these new hot-wire spatial correction schemes for streamwise Reynolds stress by applying them to new moderate Reynolds number turbulent channel flow data acquired with an array of hot-wires. Based on these results, it was determined that additional correction for end conduction effects is required and a correction for these effects is developed and combined with the Smits et al. (2011) correction. The results were found produce a marked improvement in the agreement between hot-wires of different lengths and aspect ratios and with channel flow DNS.

2 Overview of recent correction schemes

A brief overview of recently proposed spatial filtering correction schemes for $\overline{u^2}$ is provided in Table 1. In the study by Hutchins et al. (2009), a carefully matched set of hot-wires was used to measure a turbulent boundary layer from low to high Reynolds numbers. Analysis of the results indicated that the Ligrani and Bradshaw constraint on l^+ may have resulted in an underestimated error in $u^{2+} = \overline{u^2}^+/u_\tau^2$, leading to an approach to determine the actual error for large l^+ based on data from multiple facilities. Hutchins et al. found that the recommendation of $l/d > 200$ was adequate to avoid any end-conduction effects, but also found that relaxing this constraint will cause severe attenuation throughout the log layer. Examination of the measured value of the near-wall peak, $u^{2+}_{\max}$, from

Table 1 Summary of recently proposed spatial filtering corrections for $\overline{u^2}$

References	Flow type	l^+ Range	l/d Range	y^+ Range	Re Tested range
Hutchins et al. (2009)	BL, C, P	$11 < l^+ < 153$	$l/d > 200$	Peak only, $y^+ \approx 15$	$Re_\tau < 25{,}000$
Chin et al. (2009)	C	$l^+ < 30$	$l/d > 200$	Peak only, $y^+ \approx 15$	$Re_\tau = 950$ for BL[a]
Monkewitz et al. (2010)	BL	None specified[b]	Correction for l/d provided	$y^+ > 10$	$Re_{\delta^*} < 50{,}000$ for BL
Smits et al. (2011)	BL, C, P	$l^+ < 150$	None specified	Entire profile	$Re_\tau < 14{,}000$ for BL, and $Re_\tau < 3{,}000$ for P
Segalini et al. (2011)	BL, C, P	None specified	None specified	Entire profile	$Re_\tau < 14{,}000$ for BL
Chin et al. (2011)	BL, C, P	$l^+ < 60$ Demonstrated for $l^+ < 153$	None specified	Entire profile	$Re_\tau < 14{,}000$ for BL
Philip et al. (2013b)	BL, C, P	$l^+ < 40$	None specified	Entire profile	$Re_\tau < 7{,}300$ for BL and $Re_\tau < 3{,}000$ for C

BL boundary layer, *P* pipe flow, *C* channel flow

[a] While the method of Chin et al. (2009) has only been tested for a single Re, the author makes note that provided l/h is small this correction may be applied up to $Re_\tau \approx 7{,}000$

[b] Monkewitz et al. (2010) indicate that at low values of l^+ the typical correction is much larger than the error of a small wire (say, $l^+ = 6$) compared to a wire of infinitely small length and provide no lower limit on l^+. Furthermore, no high l^+ limit is mentioned

numerous turbulent boundary layers led to the determination of a relationship between measured value of $u^{2+}_{\max}$ and l^+ which follows

$$u^{2+}_{\max} = A\log_{10}(Re_\tau) - Bl^+ - C\left(\frac{l^+}{Re_\tau}\right) + D \quad (1)$$

where $A = 1.0747, B = 0.0352, C = 23.0833,$ and $D = 4.8371$. The spatial filtering effects were thus encompassed in the second and third terms, leading to a potential correction for the energy lost due to spatial filtering of

$$\left(u^{2+}_{\max}\right)_t = \left(u^{2+}_{\max}\right)_m + Bl^+ + C\left(\frac{l^+}{Re_\tau}\right) \quad (2)$$

which is independent of flow type. Here, the subscripted t indicates the true value and the subscripted m the measured value.

The correction method of Chin et al. (2009) was determined using a channel flow direct numerical simulation (DNS) data set with different spanwise filters to replicate the effects of hot-wires with limited spatial resolution. Their proposed correction takes a similar form to that of Hutchins et al. and is

$$\left(u^{2+}_{\max}\right)_t = \left(u^{2+}_{\max}\right)_m + Al^{+3} + Bl^{+2} + Cl^+ + D \quad (3)$$

with the values of the constants determined from a curve fit to the filtered DNS being $A = -1.94 \times 10^{-5}$, $B = 1.83 \times 10^{-3}, C = 1.76 \times 10^{-2},$ and $D = -9.68 \times 10^{-2}$. Although the Chin et al. correction allowed for a refinement of the l^+ values investigated, it does not encompass as wide a breadth of empirical results as the Hutchins et al. correction and hence has a lower range of validity in l^+, being limited to $l^+ < 30$.

The correction proposed by Monkewitz et al. (2010) seeks to correct for both spatial filtering effects and the thermal frequency response of hot-wires in zero-pressure gradient turbulent boundary layers. The data of Hutchins et al. (2009) and Ligrani and Bradshaw (1987) was combined to find the form of a correction due to the separate effects of l^+ and l/d which may be applied to the entire $\overline{u^2}^+$ profile for $y^+ > 10$. However the full form of the correction as proposed by Monkewitz et al. (2010) is applicable only to zero-pressure gradient turbulent boundary layers and will not be examined further in the present comparison due to our use of turbulent channel flow data.

Chin et al. (2011) revisited their DNS analysis and provided an updated correction to evaluate the missing energy lost due to spatial filtering. The revised correction modeled the missing energy, $g(\lambda_x^+, \lambda_z^+, y^+, l^+)$ for all y^+ in terms of λ_x^+ and λ_z^+, the normalized wavelengths in the streamwise and spanwise directions, respectively. This model takes the form

$$g(\lambda_x^+, \lambda_z^+, y^+, l^+) = A\exp\left(-\left[\frac{(\alpha-\alpha_0)^2}{\sigma_\alpha} + \frac{(\beta-\beta_0)^2}{\sigma_\beta}\right]\right) \quad (4)$$

and allows correction of the spectra and hence u^{2+} by allowing the missing energy to be added back into u^{2+}_m. The coefficients in Eq. 4 are not repeated here for brevity. Although Eq. 4 was formulated for filter lengths up to $l^+ = 60$, it was demonstrated to successfully correct the data of Hutchins et al. (2009) for l^+ as high as 153. A principal advantage of this correction is its ability to correct the measured energy spectra, although this capability will not be examined here.

The empirically determined Gaussian form used by Chin et al. (2011) was verified by Philip et al. (2013b) who treated spatial filtering as a linear filter applied along the span of the wire. Using a box-type filter and a generalized model of the spanwise correlation of the turbulence characterized via the length scale λ, Philip et al. found l/λ to be the most relevant parameter for the description of spatial filtering effects. A correction was developed of the form

$$\frac{u^{2+}_m}{u^{2+}_t} = \frac{2}{m}\frac{\lambda_m}{l}\left[\gamma\left(m^{-1}, \frac{l^m}{\lambda^m_m}\right) - \left(\frac{\lambda_m}{l}\right)\gamma\left(2m^{-1}, \frac{l^m}{\lambda^m_m}\right)\right] \quad (5)$$

where γ is the incomplete Gamma function and the Reynolds number and y^+ dependence of λ are modeled through m and λ_m. This analysis was further adapted for two-wire probes in Philip et al. (2013a).

The spatial correction of Smits et al. (2011) is based on the attached eddy hypothesis of Townsend (1976). The data of Hutchins et al. (2009), Ng et al. (2011), and the results of Chin et al. (2009) were combined with a functional form of

$$u^{2+}_t = [M(l^+)f(y^+) + 1]u^{2+}_m \quad (6)$$

where M and f are functions describing the dependency of the spatial filtering on wire viscous length and wall distance, respectively. These functions were given as

$$M(l^+) = A\tanh(\xi l^+)\tanh(\zeta l^+ - E)/u^{2+}_{\max} \quad (7)$$

and

$$f(y^+) = \frac{15 + \ln 2}{y^+ + \ln[e^{(15-y^+)} + 1]} \quad (8)$$

where $A = 6.13, E = -1.26 \times 10^{-2}, \xi = 5.6 \times 10^{-2}$ and $\zeta = 8.6 \times 10^{-3}$. This correction is applicable over a wide range of viscous wire lengths, $0 < l^+ < 150$, all wall distances, and can be applied to boundary layer, channel, and pipe flows with apparent success.

The correction proposed by Segalini et al. (2011) employs a unique approach to correcting the Reynolds stress using two single hot-wires of different lengths to construct the two-point correlation function and hence

attenuation due to wire length of the true Reynolds stress, while simultaneously producing an estimate of the Taylor microscale. While this approach has the added requirement of using two hot-wires of differing length at the same flow conditions, its application is not limited to canonical wall-bounded flow and it is free from fitting parameters, assuming only statistically homogeneous flow along the wire. Good results were found using both the DNS of Schlatter and Örlü (2010) and the data of Hutchins et al. (2009) to evaluate this approach. Further modifications to this correction for higher-order moments are provided in Talamelli et al. (2013).

To compare these corrections, we applied them to a data set acquired over a range of $l^+, l/d$ and Re_τ in a turbulent channel flow. The corrected results were evaluated by both examining the ability of the correction to collapse Reynolds stress profiles acquired with different hot-wires and the same flow condition as well as by comparison to the DNS results of Hoyas and Jiménez (2006) and Lozano-Durán and Jiménez (2014). Due to the calibration of the Monkewitz et al. (2010) correction for turbulent boundary layers, we will concentrate our comparison to the Hutchins et al. (2009), Chin et al. (2009, 2011), Smits et al. (2011), Segalini et al. (2011), and Philip et al. (2013b) corrections.

3 Experimental apparatus

The experiments were conducted in the turbulent channel flow facility located in the Experimental Fluid Dynamics Laboratory at the University of Kentucky. A schematic of the facility is provided in Fig. 1. This facility has been designed to produce fully developed turbulent, plane Poiseuille flow at the channel centerline. The channel had a half height of $h = 50.8$ mm and an aspect ratio of 9:1 to ensure quasi-2D flow at the centerline (Zanoun and Durst 2003). This allowed for Reynolds numbers of up to $Re_h = 94{,}000$, and $Re_\tau = 4{,}200$ based on area averaged velocity, U_b, and u_τ respectively. A boundary layer trip consisting of a 50-mm-wide section of 120-grit sand paper followed by a 100-mm-wide section of 60-grit sandpaper was located at the channel inlet. The distance from the channel inlet to the test section was 246 h, allowing the turbulence to reach a fully developed state naturally (Monty 2005) before entering the channel test section. The test section was 24 h long, with an instrumentation plug located at its center. Following the test section, an additional 12-h-long conditioning section maintained a consistent pressure gradient inside the test section. Surface roughness was measured on a sample of the test section wall using a stylus surface profilometer. The sample was found to have an rms roughness height of 268 nm along the grain of the aluminum and 334 nm across the grain, approximately 2.5 % of the viscous length at the highest Reynolds number reported here.

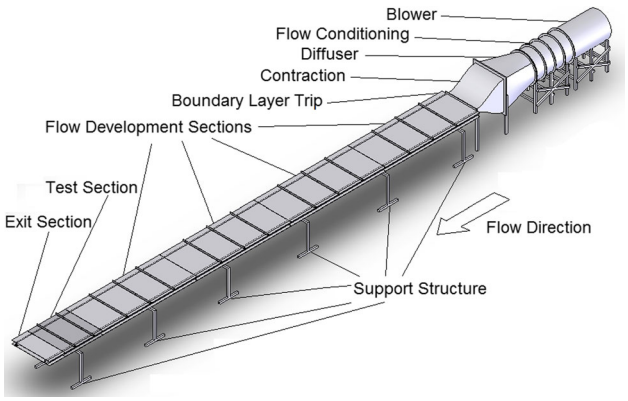

Fig. 1 Schematic of the turbulent channel flow facility used in this study

The hot-wire probes used in this study were constructed by soldering Wollaston wire onto Auspex boundary-layer-type hot-wire prongs. This wire was then etched to specific sensing lengths in the range $l = 0.50$ to 1.65 mm corresponding to l/d between 200 and 603. The probe was driven by a Dantec Streamline Constant Temperature Anemometer (CTA) system at an overheat ratio of 1.5 to 1.6 to ensure very small probe drift over the course of an experiment and cut-off frequency of $f_c > 35$ kHz as determined by a square wave test. To traverse the probes in the channel, a nano-stepping traverse with a high-accuracy linear encoder was used (500 nm resolution and ± 3 µm accuracy). The hot-wire could thus be accurately positioned relative to the wall using an electrical contact switch which triggered at the initial probe position for each measurement. The distance of the probe to the wall at the initial location was determined with a Titan Tool Supply Z-axis ZDM-1 microscope with an accuracy of ± 5 µm.

Calibration of the probes took place in-situ, directly prior to and following a measurement run using a Pitot probe located at the channel centerline. Both the pre- and post-calibrations and the actual run bridge voltages were corrected in post-processing for any temperature variations (Tavoularis 2005) measured within the channel by a thermistor probe. Measured bridge voltages were filtered at 30 kHz and digitized by a National Instruments PCI-6123 data acquisition card with 16-bit resolution. The acquisition time for each run, t_s, was selected at each Re_τ to capture at least 100 instances of the largest structures (which have been found to be $\mathcal{O}(20h)$, Monty et al. 2007) to ensure converged statistics. Following acquisition, a fourth-order polynomial was used to fit the calibration curves. The largest allowed probe drift between pre-calibration and post-calibration was 0.7 % of the centerline velocity.

Table 2 Nominal parameters for hot-wire probes used in this study and corresponding figure symbol

Symbols	l (mm)	d (μm)	Material type	l^+ @ Re_τ					
				700	1,000	1,600	2,200	3,000	4,200
▽	0.50	2.5	Pt	N/A	N/A	N/A	18	27	37
◇	0.56	2.5	Pt-Rh	7.0	11	16	23	N/A	N/A
	0.90	2.5	Pt-Rh	11	17	25	37	N/A	N/A
◯	0.90	5.0	Pt -Rh	11	17	25	37	N/A	N/A
□	1.49	2.5	Pt-Rh	18	29	42	60	N/A	N/A
	1.49	5.0	Pt-Rh	18	29	42	60	N/A	N/A
★	1.65	5.0	Pt-Rh	N/A	N/A	N/A	61	87	121

Table 2 contains the nominal parameters for each hot-wire. Measurements were conducted at six Reynolds numbers to produce a variation in l^+ from 5.5 to 121. One important consideration when designing the experiment was the viscous time scale, t^+. Hutchins et al. (2009) found that $t^+ \approx 3$ will adequately resolve the temporal fluctuations to an error of <0.1 %. The 30-kHz cutoff filter employed in these experiments imposed a constraint on these measurements, but for all cases $t^+ < 3$. Thus, even at the highest Reynolds numbers, the error due to temporal resolution is expected to be very small.

To determine the friction velocity, two methods were used. The channel facility is outfitted with static pressure taps every 12 h along its length which allow determination of the pressure loss in the fully developed section of the channel using a simple momentum balance (see, for example Pope 2000). One alternate method of determining the friction velocity is to use the Clauser chart method (Clauser 1956). Both approaches were found to be in good agreement, to within less than 3 %. However, the Clauser chart method was found to result reduced variation in u_τ at the same Re_τ compared to the pressure drop method due to the relatively low sensitivity of the pressure transducer used for the static pressure measurements. Therefore, here we will use the value of u_τ determined using the Clauser chart approach, which was found to vary between profiles by ± 1 % to ± 3 % at each measured Reynolds number.

4 Uncorrected results

The Reynolds stress profiles without corrections applied are plotted in Fig. 2. The effects of spatial filtering are readily apparent with increasing Re_τ (reducing viscous length scale) and as wire length is increased. To further highlight the scatter introduced by wire dimension effects, the peak in Reynolds stress, $u^{2+}_{\max}$, is provided in Fig. 3 and compared to the values extracted from the turbulent channel DNS of Hoyas and Jiménez (2006) and Lozano-Durán and Jiménez (2014). Here, the effects of spatial filtering are clearly discernible, and the measured $u^{2+}_{\max}$ is consistently lower than the DNS values and increasingly diverges from the DNS trend as the Reynolds number increases and viscous length decreases.

The results of Figs. 2 and 3 clearly reflect the sensor-dependent bias introduced into the measurements of u^{2+}. For example, at $Re_\tau = 2{,}000$, at $l^+ = 61$ a 40 % difference was observed between the measured and DNS value of $u^{2+}_{\max}$.

5 Comparison of spatial filtering corrections

We now compare results from the different corrections developed to counter the spatial filtering effects demonstrated in Figs. 2 and 3. First, we examine the Hutchins et al. and Chin et al. corrections, which are both intended to correct the magnitude of the near-wall peak. The measured values presented in Fig. 3 are shown corrected using the Hutchins et al. correction in Fig. 4a and using the Chin et al. correction in Fig. 4b. Noting that the Chin et al. correction is described as being valid only for $l^+ < 30$, data points outside this range are presented as gray symbols.

The results are surprisingly different between the two corrections. The Hutchins et al. correction corrects $u^{2+}_{\max}$ to with a scatter of $\pm \sim 4$ % centered on the DNS trend for $Re_\tau < 2{,}000$. For $Re_\tau > 2{,}000$, the corrected values appear to deviate from trend exhibited by the DNS. The Chin et al. correction also corrects the results to approximately the same level of agreement ($\pm \sim 4$ %), at least for cases where $l^+ < 30$, as illustrated in Fig. 4b. However, the trend exhibited by the corrected results is clearly different from that of Hutchins et al. correction, with an increased Re_τ dependence observed. When l^+ exceeded 30, the correction began to fail due to the third-order polynomial used for l^+ achieving a maximum and reversing its trend. As a result, the $l^+ = 121$ wire at $Re_\tau = 4{,}200$ corrected to a negative value of u^{2+} (and therefore not appearing in Fig. 4b).

These first two corrections applied have limited utility due to being confined to the near-wall peak. Therefore, the corrections of Smits et al. (2011), Segalini et al.

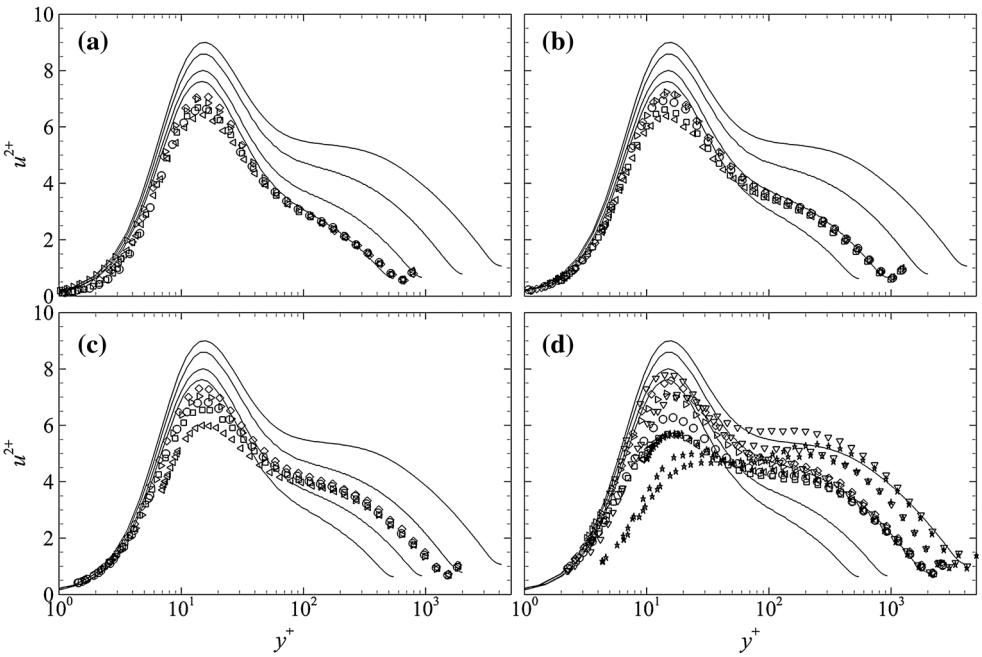

Fig. 2 Measured profiles of u^{2+} plotted in inner coordinates. DNS results of Hoyas and Jiménez (2006) at $Re_\tau =$ 550, 950 and 2,000 and Lozano-Durán and Jiménez (2014) at $Re_\tau = 4{,}200$ are plotted as a *solid line*. **a** $Re_\tau = 700$; **b** $Re_\tau = 1{,}000$; **c** $Re_\tau = 1{,}600$; and **d** $Re_\tau \geq 2{,}200$. *Symbols* as in Table 2

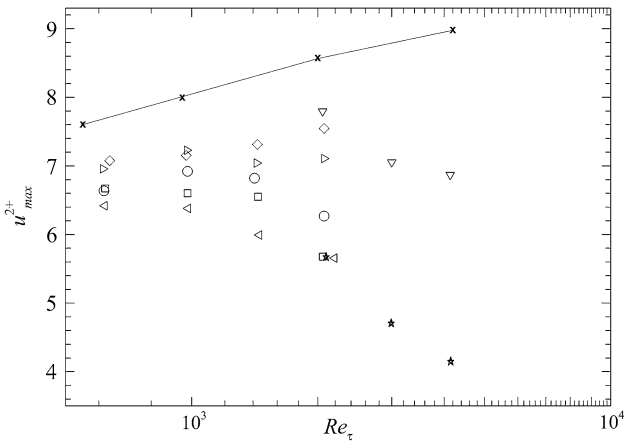

Fig. 3 Measured maximum in streamwise Reynolds stress as a function of Reynolds number. *Symbols* as in Table 2. *Solid line* and *times symbol indicate* values from Hoyas and Jiménez (2006) and Lozano-Durán and Jiménez (2014) turbulent channel flow DNS

(2011), Chin et al. (2011), and Philip et al. (2013b) are more useful due to their ability to correct the entire profile. The u^{2+} profiles shown in Fig. 2 following application of the Smits et al. correction are shown in Fig. 5. The effectiveness of these corrections becomes readily apparent when comparing Figs. 2, 3, 4, and 5. Although there are some profiles which are not in complete agreement with the others, in general, the correction successfully collapses the data from the disparate wire lengths at nearly all y^+ locations and results in good agreement with the DNS profiles at corresponding Re_τ.

The agreement between the data sets can be examined in greater detail by looking at the corrected $u^{2+}_{\max}$ values, shown in Fig. 4c. Here, it can be observed that the resulting values agree to within the same level of agreement as the Hutchins et al. (2009) and Chin et al. (2009) corrections ($\pm \sim 4$ %). However, as observed with the Chin et al. (2009) correction, the values of $u^{2+}_{\max}$ are typically lower than that exhibited by the DNS trend. For $Re_\tau > 2{,}000$, the values of $u^{2+}_{\max}$ are in better agreement than they were following application of the Hutchins et al. correction, and better follow the trend expected from the DNS results.

We next examine the correction of Segalini et al. (2011), with the u^{2+} profiles corrected using this approach provided in Fig. 6. As this correction requires two values measured at the same location and Re_τ but having different wire length, we used one hot-wire as a consistent reference to correct the remaining hot-wires.

Two observations are readily apparent when examining the results presented in Fig. 6. The first is that application of the correction to the $l = 0.56$ mm probe profile is clearly unsuccessful, potentially due to the relative importance of spatial filtering to other sources of error being small, resulting in the correction compensating for error due to other sources. However, if we ignore that particular profile, the second observation which can be immediately made is that the remaining profiles exhibit improved collapse relative to the other corrections.

This collapse is particularly evident in the corrected values of $u^{2+}_{\max}$, shown in Fig. 4d. Neglecting the $l =$ 0.56 mm probe result, for $Re_\tau < 2{,}000$ the corrected $u^{2+}_{\max}$ values are remarkably close to the trend exhibited by the DNS and within $\pm \sim 3$ % of each other.

Using the collapse of the data on the DNS trend as a metric for success of the correction, it would appear that this correction is most successful. However, this could be

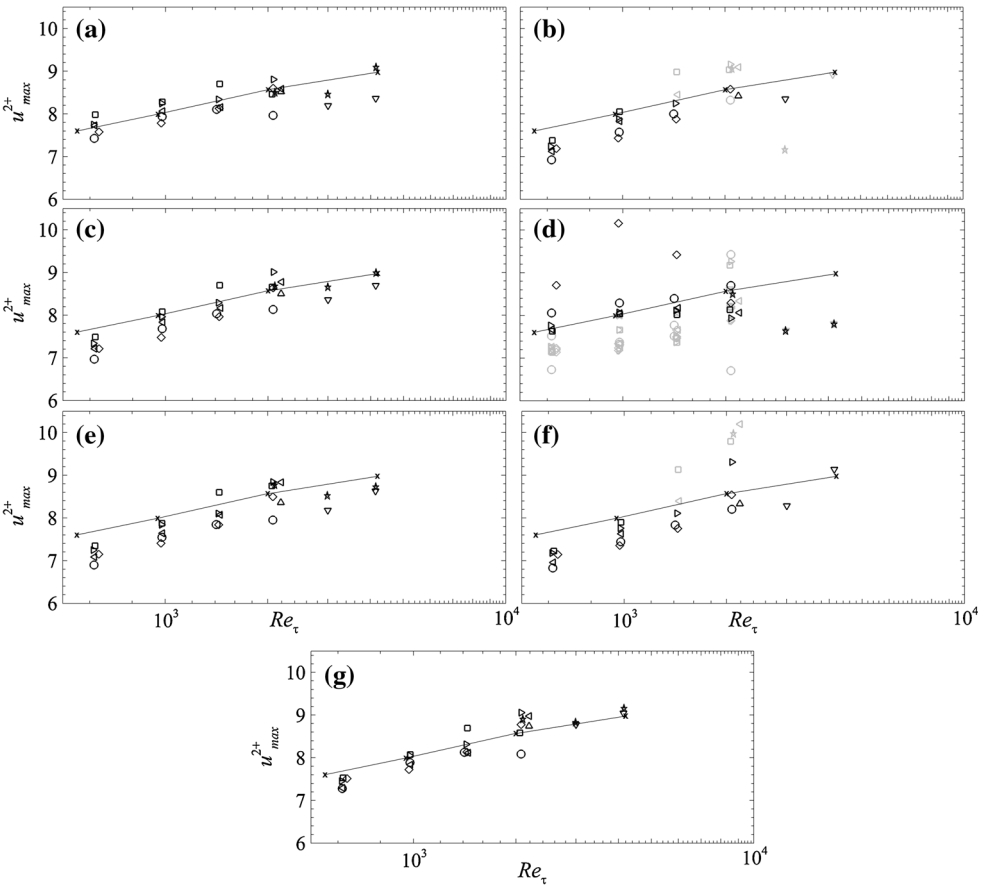

Fig. 4 Measured maximum in streamwise Reynolds stress as a function of Reynolds number corrected using the: **a** Hutchins et al. (2009) correction; **b** Chin et al. (2009) correction; **c** Smits et al. (2011) correction; **d** Segalini et al. (2011) correction; **e** Chin et al. (2011) correction; **f** Philip et al. (2013b) correction; and **g** Smits et al. (2011) correction modified to account for end conduction effects as described in Sect. 6. *Symbols* as in Table 2. *Solid line* and *times symbol* indicate values from Hoyas and Jiménez (2006) and Lozano-Durán and Jiménez (2014) DNS

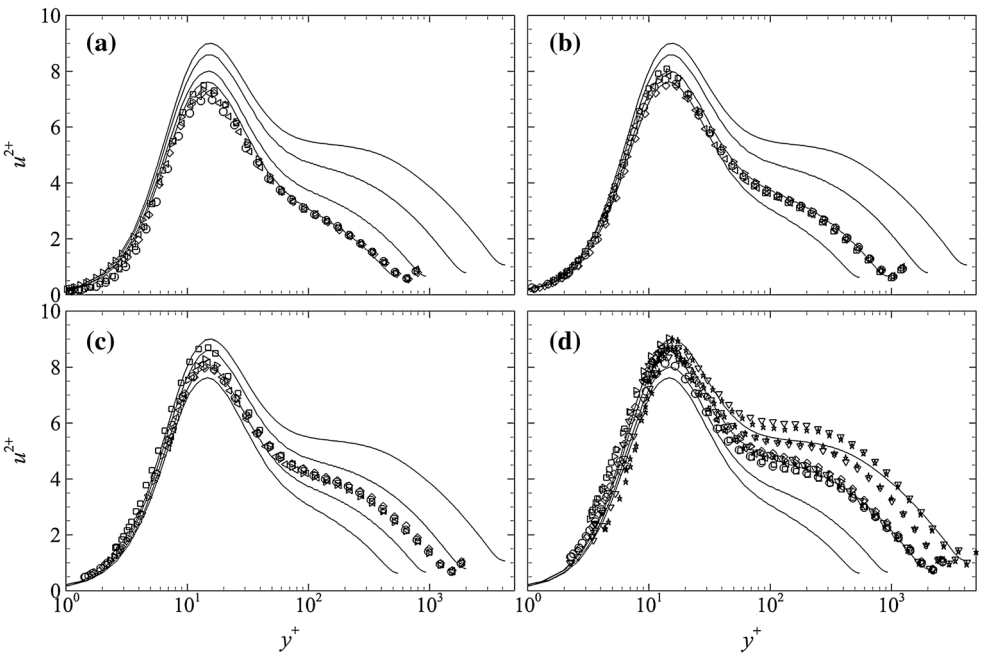

Fig. 5 Measured profiles of u^{2+} corrected using the Smits et al. (2011) correction, plotted in inner coordinates. DNS results of Hoyas and Jiménez (2006) at $Re_\tau = 550$, 950 and 2,000 and Lozano-Durán and Jiménez (2014) at $Re_\tau = 4{,}200$ are plotted as a *solid line*. **a** $Re_\tau = 700$; **b** $Re_\tau = 1{,}000$; **c** $Re_\tau = 1{,}600$; and **d** $Re_\tau \geq 2{,}200$. *Symbols* as in Table 2

fortuitous, as the corrected profiles in Fig. 6 lie above the DNS profiles for $y^+ > 15$, and the improved collapse is due to the use of a consistent reference probe to correct the different length wires. To illustrate this second point, the corrections were repeated with all possible combinations of probes, and the results are also shown as gray symbols on Fig. 4d. When all combinations of probes are considered, the resulting trend is similar to the Smits et al. corrected

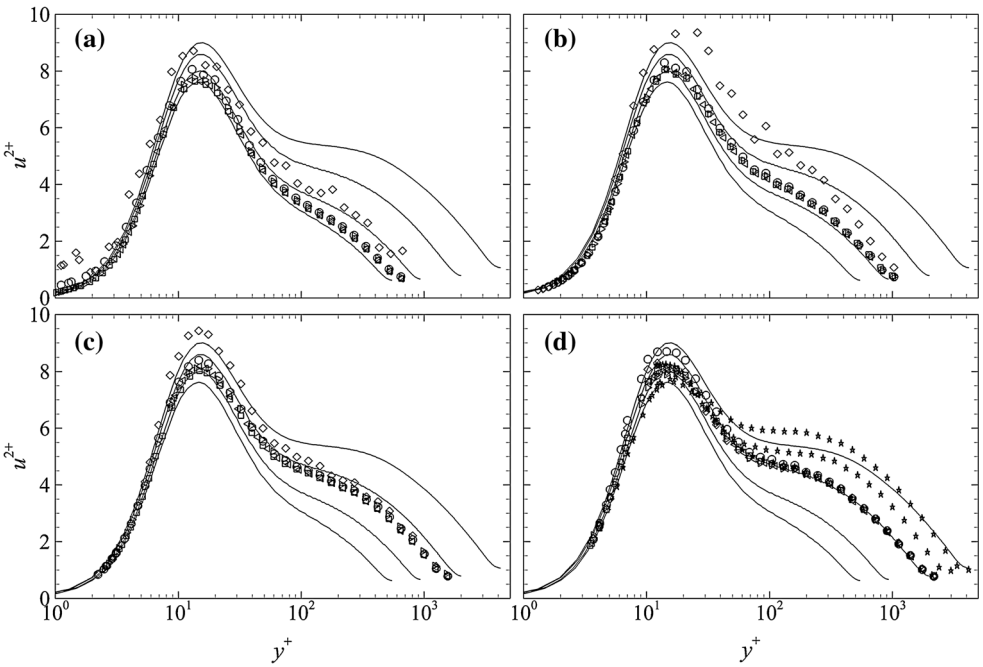

Fig. 6 Measured profiles of u^{2+} corrected using the Segalini et al. (2011) correction, plotted in inner coordinates. DNS results of Hoyas and Jiménez (2006) at $Re_\tau = 550, 950$ and 2,000 and Lozano-Durán and Jiménez (2014) at $Re_\tau = 4{,}200$ are plotted as a *solid line*. **a** $Re_\tau = 700$; **b** $Re_\tau = 1,000$; **c** $Re_\tau = 1{,}600$; and **d** $Re_\tau \geq 2{,}200$. *Symbols* as in Table 2

results, however, with an increased scatter and more outliers.

One possible source of the increased scatter with this correction is that the two-point correlation used to estimate the true value of u^{2+} requires that the wires were measuring under the exact same conditions. Any differences in the flow environment, or even any experimental error in one of the calibration curves, would be amplified in the corrected value of u^{2+}. Hence, it would be expected that improved results would be achieved if both wires were measuring simultaneously. Another note on this correction is that it was found that minimization of the two-point correlation function was very sensitive to initial conditions. However, this will depend mainly on the least squares minimization function used to find solutions to the two-point correlation function. The success of this correction will be dependent on the quality of the source profiles and small errors can be amplified by the correction.

The next correction which will be examined is that of Chin et al. (2011) and the corrected profiles of u^{2+} are shown in Fig. 7.[1] The resulting profiles are comparable to those corrected using Smits et al. (2011) with two notable exceptions. The first being improved agreement between the profiles at high Reynolds numbers for $y^+ < 15$ and the second being the $l^+ = 121$ profile at $Re_\tau = 4{,}200$ appearing under-corrected in the range $20 < y^+ < 700$, suggesting less reliability at high values of l^+. Note that similar behavior can be observed when closely examining Fig. 8 of Chin et al. (2011) at $l^+ = 153$ and $Re_\tau = 14{,}000$. The similarity between the Chin et al. (2011) and Smits et al. (2011) corrected results is further reflected in the corrected values of $u^{2+}_{\max}$, shown in Fig. 4e.

Finally, the u^{2+} profiles corrected using the Philip et al. (2013b) correction are presented in Fig. 8. For $Re_\tau < 1{,}600$ the results were comparable to those corrected using the Smits et al. (2011) and Chin et al. (2011). However for increasingly large l^+ the results were under-corrected, most notably when $l^+ > 35$. This similarity to the Chin et al. (2011) and Smits et al. (2011) corrected results and over-correction at higher l^+ is further reflected in the corrected values of $u^{2+}_{\max}$, shown in Fig. 4e.

Thus, most of the corrections produce collapse in u^{2+} measured with different probes at the same conditions to within the roughly the same level of agreement, $\pm \sim 4$ %. This is consistent with the validations presented in each of the papers describing the corrections whereby the metric for success is the agreement between the corrected results from two or more probes measured under the same conditions. To provide a more detailed assessment of the differences between the corrections, the profile measured by the $l = 0.95$ mm, $d = 2.5$ μm probe at $Re_\tau = 1{,}000$ corrected using the different approaches is compared to the DNS results of Hoyas and Jiménez (2006) at $Re_\tau = 950$ in Fig. 9. Since the same wire can be combined with different probes for the Segalini et al. (2011) correction, the combination which best agreed with the DNS is shown as symbols, and the remaining combinations are shown as gray lines.

[1] Note that to reproduce Fig. 4 in Chin et al. (2011), we had to change the denominator of the first term in their Eq. 11 from $(3.35y^+)^{3.25}$ to $3.35(y^+)^{3.25}$.

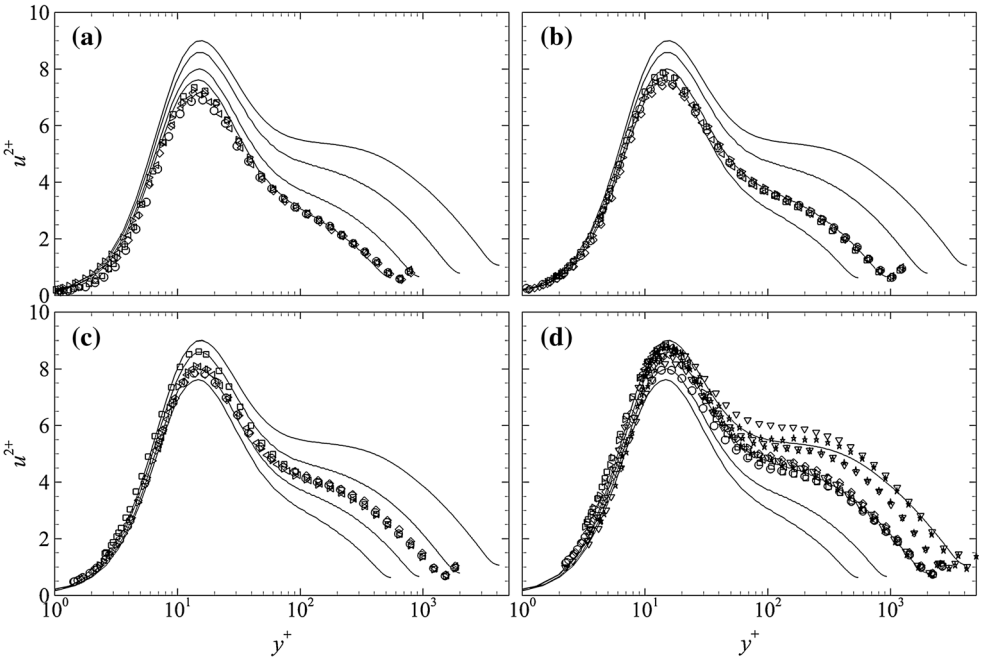

Fig. 7 Measured profiles of u^{2+} corrected using the Chin et al. (2011) correction, plotted in inner coordinates. DNS results of Hoyas and Jiménez (2006) at $Re_\tau = 550$, 950 and 2,000 and Lozano-Durán and Jiménez (2014) at $Re_\tau = 4{,}200$ are plotted as a *solid line*. **a** $Re_\tau = 700$; **b** $Re_\tau = 1{,}000$; **c** $Re_\tau = 1{,}600$; and **d** $Re_\tau \geq 2{,}200$. *Symbols* as in Table 2

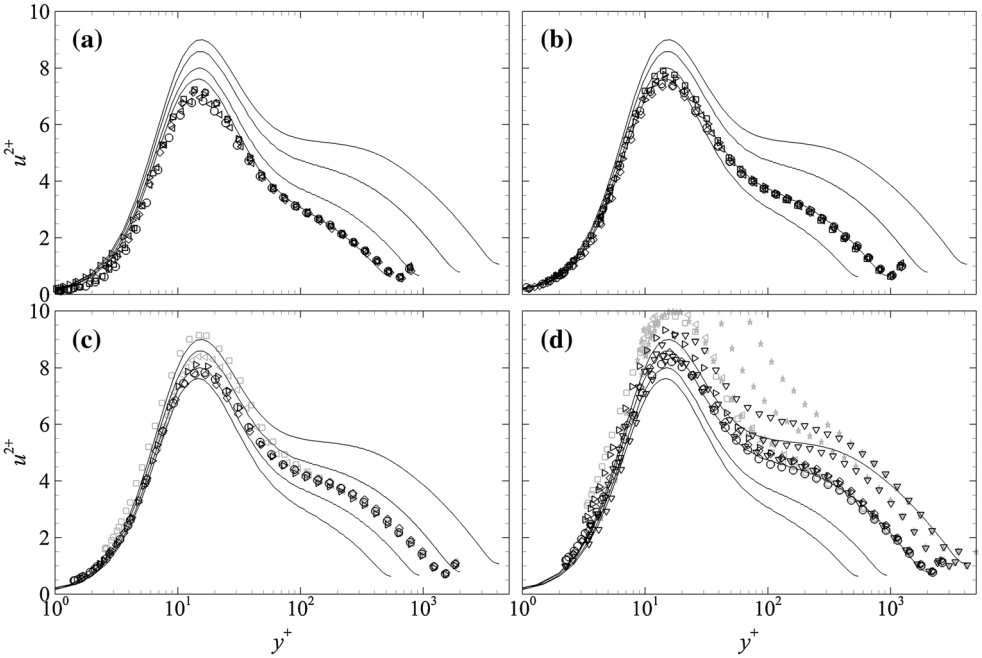

Fig. 8 Measured profiles of u^{2+} corrected using the Philip et al. (2013b) correction, plotted in inner coordinates. *Symbols* shown in *gray* represent profiles where l^+ was outside the stated range of validity for the correction. DNS results of Hoyas and Jiménez (2006) at $Re_\tau = 550$, 950 and 2,000 and Lozano-Durán and Jiménez (2014) at $Re_\tau = 4{,}200$ are plotted as a *solid line*. **a** $Re_\tau = 700$; **b** $Re_\tau = 1{,}000$; **c** $Re_\tau = 1{,}600$; and **d** $Re_\tau \geq 2{,}200$. *Symbols* as in Table 2

Due to end wall effects, the DNS may not accurately represent the true value of u^{2+} for this facility. However, we found that for $y^+ > 80$, there is quite good agreement between the DNS and the results corrected by the Smits et al. (2011), Chin et al. (2011) and Philip et al. (2013b) corrections. The Segalini et al. (2011) corrected results were generally higher than the DNS for $y^+ > 25$ and were consistently lower than the DNS for $y^+ < 15$. The sensitivity of this correction to the probe combination selected is apparent. Close inspection of the remaining three corrections shows that the shape of the near-wall peak is slightly affected by the correction selected. Although there was very little difference between the Chin et al. (2011) and Philip et al. (2013b) corrected results, which were slightly lower than the DNS for $y^+ < 27$, the Smits et al. (2011) corrected profile were slightly lower than the DNS for $15 < y^+ < 50$. Due to the possibility of propagation of error from other sources, it is not possible to know which of these three corrections is the most accurate. However, all three of these corrections were within 3 % of the DNS at $y^+ = 15$, representing a remarkable level of agreement given the very different approaches used to devise each correction.

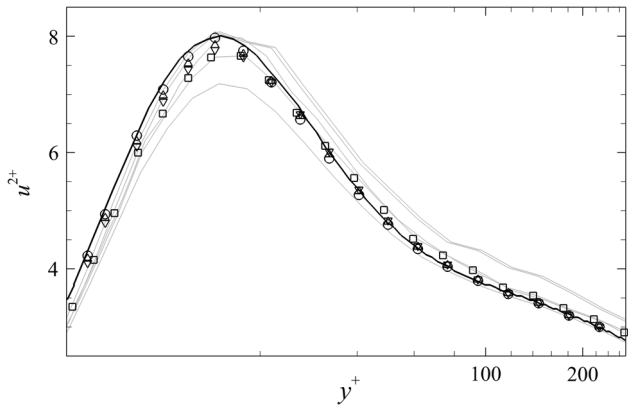

Fig. 9 $l = 0.9\,\text{mm}\; d = 2.5\,\mu\text{m}$ wire results at $Re_\tau = 1{,}000$ corrected using: (*circle*) Smits et al. (2011; *square*) Segalini et al. (2011; *triangle*) Chin et al. (2011); and (*inverted triangle*) Philip et al. (2013b) corrections. *Gray lines* indicate results from Segalini et al. (2011) correction determined using different probes as reference. *Black line* indicates profile from $Re_\tau = 950$ from Hoyas and Jiménez (2006)

6 Modification for end conduction effects

Excepting the Hutchins et al. correction, the corrected values of $u^{2+}_{\max}$ were typically found to correct to slightly below the DNS value at equivalent Re_τ, most noticeably for $Re_\tau < 2{,}000$. However, the corrections employed here focus solely on the parameter l^+ to characterize the spatial filtering effects, assuming uniform filtering along the wire and negligible end conduction effects. These end conduction effects can be characterized by a 'cold length' representing the length of wire effectively cooled by the support (Perry 1982). The cold length is defined as

$$l_c = d\sqrt{\frac{k_w \varphi}{4 k_a Nu}} \tag{9}$$

where k_w and k_a are the thermal conductivity of the wire and air evaluated at the film temperature, Nu the Nusselt number and φ the overheat ratio of the wire (Tavoularis 2005). For a particular physical length of wire, a shorter cold length implies a larger sensing length and hence greater susceptibility to spatial filtering. We also note that the cold length will exhibit Reynolds number sensitivity through Nu and hence introduce additional wall-normal and Reynolds number dependence into the spatial filtering experienced by the wire.

The present data set was acquired at relatively low overheat ratios of $\varphi = 1.5$ to 1.6 and using Pt-Rh ($k_w = 38\,\text{Wm}^{-1}\,\text{K}^{-1}$) wires. We therefore can anticipate that the cold length of these wires will be shorter than that for the $\varphi = 1.8$, Pt ($k_w = 72\,\text{Wm}^{-1}\,\text{K}^{-1}$) hot-wires used by Hutchins et al. (2009) and Chin et al. (2011), the data sets used to formulate and validate the corrections examined in the previous section (with the notable exception being the Hutchins et al. correction). Therefore, it would appear that modifications are required to allow the corrections to account for non-uniform heat distribution and end conduction effects.

We introduce an effective wire length, $l_{eff} = l - 2l_c$, to describe the actual active length of the wire and account for the modification to the wire active length due to end conduction. Furthermore, as noted in Hultmark et al. (2011), the original recommendation by Ligrani and Bradshaw to avoid end conduction effects using $l/d > 200$ is valid only for platinum wires at "typical" velocities and atmospheric pressure. Hultmark et al. propose a new parameter to characterize end conduction effects which accounts for many of the variables which could affect the response of the probe

$$\Gamma = \varphi \frac{l}{l_c}. \tag{10}$$

Figure 10 is adapted from Hultmark et al. (2011) and shows the dependency of $\overline{u^2}_m/\overline{u^2}_t$ on Γ using the Ligrani and Bradshaw data at $y^+ \approx 15$. These results can be represented by the function

$$\left.\frac{\overline{u^2}_m}{\overline{u^2}_t}\right|_{y^+\approx 15} = 1 - g(\Gamma) \tag{11}$$

where

$$g(\Gamma) = 20(\Gamma + 2.7)^{-2.2} \tag{12}$$

as illustrated using the solid line in Fig. 10.

This expression can thus be used to correct for aspect ratio effects present in hot-wire measurements at $y^+ \approx 15$. However, noting that end conduction acts through a degradation of the frequency response of the probe, the degree to which the probe's response is damped due to end conduction will be dependent on the frequency content of the turbulence and hence exhibit y^+ dependance. A simple approach to extend $g(\Gamma)$ to other wall-normal locations can be made by assuming separable variables and extending the wall-normal dependence of the turbulence described by $f(y^+)$ in the Smits et al. (2011) correction to the frequency domain using Taylor's hypothesis. Thus

$$\frac{\overline{u^2}_m}{\overline{u^2}_t} = 1 - g(\Gamma) f(y^+) \overline{U}/\overline{U}_{\max} \tag{13}$$

where $\overline{U}$ is the local mean velocity and $\overline{U}_{\max}$ is the mean velocity at $y^+ = 15$. Thus, Eq. 13 allows the correction for end conduction effects throughout the wall layer.

To demonstrate these modifications for end conduction effects, we incorporated them into the Smits et al. (2011) correction. The resulting form of the correction is

$$u_t^{2+} = \left[\frac{M(l_{eff}^+)f(y^+)+1}{(1-f(y^+)\frac{\overline{U}}{\overline{U}_{\max}}g(\Gamma)}\right]u_m^{2+}. \quad (14)$$

It was found that letting $E = -0.05$ was sufficient to convert the empirical function $M(l^+)$, given by Eq. 7, to $M(l_{eff}^+)$.

The u^{2+} profiles following application of this correction are presented in Fig. 11. Although the corrected results appear largely unchanged when compared to the original Smits et al. corrected results of Fig. 5, the subtle differences become more apparent when examining $u_{\max}^{2+}$ shown in Fig. 4g. Whereas the standard Smits et al. correction collapsed $u_{\max}^{2+}$ to within ±4 %, with the modifications for end conduction effects, this improves to ±3 %.

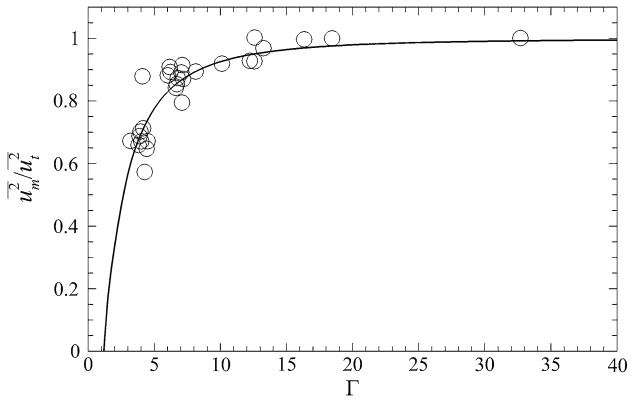

Fig. 10 The dependency of maximum measured streamwise Reynolds stress on end conduction effects measured by Ligrani and Bradshaw (1987). *Solid line* is Eq. 11. (figure adapted from Hultmark et al. 2011)

Considering that the 1–3 % scatter in the estimates of u_τ would propagate to a 2–6 % scatter in u^{2+}, it appears that the scatter observed in Fig. 4g can be attributed to uncertainty in u_τ rather than inaccuracy in the correction. In addition to improved collapse of the different length probes for $Re_\tau \leq 2{,}000$, there is also better agreement between the two probes which were used to measure for $Re_\tau > 2{,}000$ and closer agreement with the DNS trend, particularly for $Re_\tau \geq 1{,}000$.

To demonstrate the suitability of these modifications for other data sets, they were also applied to the measurements of Hultmark et al. (2010) for pipe flow at $Re_\tau < 3{,}200$ using two different sets of hot-wires. The first set had $l/d = 160$, with a constant physical length and thus l^+ increased with Re_τ. The second set used hot-wires with the sensing length adjusted such that $l^+ = 20$ at each Reynolds number. The results from this study suggested that, in pipe flows, the magnitude of the near-wall peak is invariant with Re_τ. This was in contrast to observations from channel flow DNS (for example Hoyas and Jiménez 2006) and boundary layers (for example DeGraaff and Eaton 2000; Hutchins et al. 2009) which indicate that the near-wall peak increases with Re_τ. As detailed in Örlü and Alfredsson (2013), this was also in contrast to the DNS results of Wu and Moin (2008), and observations from recent low Reynolds numbers experiments (for example Ng et al. 2011) which found the Re_τ dependence of $u_{\max}^{2+}$ to be similar to that of channel flow. Despite these inconsistencies, the Hultmark et al. observations have remained largely intact through extensions of the original study to higher Re_τ using MEMS-based hot-wires (Hultmark et al. 2012, 2013) with only a moderate increase in $u_{\max}^{2+}$ evident with Re_τ.

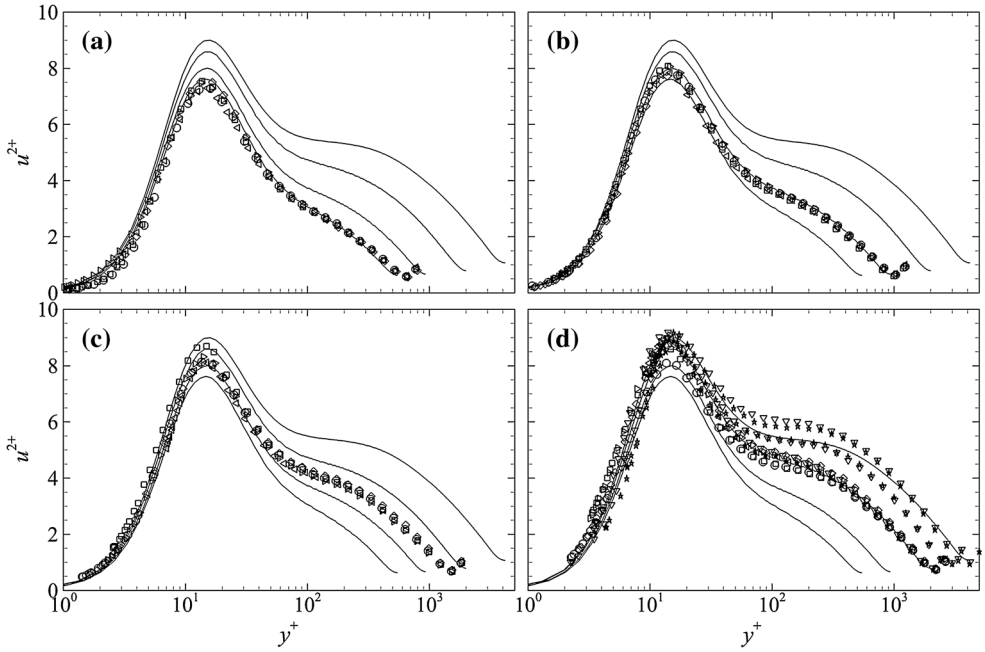

Fig. 11 Measured profiles of u^{2+} corrected using the Smits et al. correction modified to account for end conduction effects. DNS results of Hoyas and Jiménez (2006) at $Re_\tau = 550$, 950 and 2,000 and Lozano-Durán and Jiménez (2014) at $Re_\tau = 4{,}200$ are plotted as a *solid line*. **a** $s\,Re_\tau = 700$; **b** $Re_\tau = 1{,}000$; **c** $Re_\tau = 1{,}600$; and **d** $Re_\tau \geq 2{,}200$. *Symbols* as in Table 2

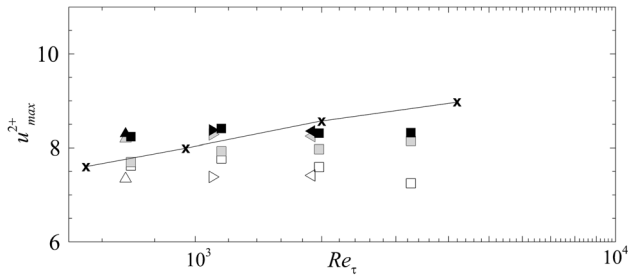

Fig. 12 Maximum measured streamwise Reynolds stress from pipe flow investigation of Hultmark et al. (2010). *Hollow symbols* identify the original data, *gray symbols* identify the same data corrected for spatial filtering effects only, *black symbols* identify the same data corrected for both spatial filtering and end conduction effects: *triangle* $l = 1.8$ mm, $d = 2.5$ μm; *right pointing triangle* $l = 1.65$ mm, $d = 2.5$ μm; *left pointing triangle* $l = 0.675$ mm, $d = 2.5$ μm; and *square* $l = 0.4$ mm, $d = 2.5$ μm

As expected, and shown in Fig. 12, the measured value of the near-wall peak for the Hultmark et al. (2010) data shows strong dependence on l^+ with the two different sets of wires measuring different values at each value of Re_τ. Interestingly, when the standard Smits et al. spatial filtering correction was applied, the agreement between the probes actually decreased. However, when the additional modifications for end conduction effects were incorporated, the two sets of wires were found to have nearly perfect agreement in the values of $u^{2+}_{\max}$ and no noticeable increase in Re_τ dependence. Thus, the independence of the near-wall peak with increasing Re_τ observed by Hultmark et al. cannot be attributed to spatial filtering or end conduction effects.

7 Conclusions

An investigation was conducted using new turbulent channel flow data investigating the effectiveness of several hot-wire spatial resolution corrections for the streamwise Reynolds stress measured in wall-bounded turbulence. When used within their suggested range of l^+, all corrections were found to be effective in that they all collapsed the results from different wires to within the same $\pm\sim 4$ %. Given the varied nature of the corrections, the success and agreement of the corrections was notable.

Some weaknesses in the corrections were also observed during their application. The Hutchins et al. (2009) and Chin et al. (2009) corrections are limited to the near-wall peak, and the Philip et al. (2013b) correction was found to significantly over-correct for $l^+ > 35$. The Segalini et al. (2011) correction, which utilizes results from two different spatially filtered probes, exhibited strong sensitivity to the probe combination employed, resulting in amplification of small experimental uncertainties. However, it should also be noted that this approach is the only one which is valid in non-canonical wall-bounded flow.

For canonical cases, the Chin et al. (2011) correction is the only one which currently offers the ability to correct measured spectra. However, it should be noted that for the highest l^+ case, this correction was found to under-correct within a limited y^+ range within the profile, suggesting that the range of validity ends somewhere between an l^+ of 90 and 120.

Comparison between the corrected results and DNS suggested that, even with hot-wires where $l/d \geq 200$, additional corrections were necessary to account for end conduction effects. A simple correction for these effects was devised using the Γ parameter developed by Hultmark et al. (2011) and was incorporated into the Smits et al. (2011) correction. When this correction was applied, it produced further reduction in the scatter of the corrected results and resulted in improved agreement with the DNS, particularly at the highest Reynolds numbers measured. The correction was also successfully demonstrated using the pipe flow measurements of Hultmark et al. (2010). The corrected results preserved the Re_τ invariance of the near-wall peak, which had been observed in the original data, indicating that this observed invariance could not be attributed to spatial filtering or end-conduction effects.

Acknowledgments Support for M.Miller was provided by a NASA Office of the Chief Technologist Space Technology Research Fellowship (Grant No. NNX12AN20H).

References

Bailey SCC, Kunkel GJ, Hultmark M, Vallikivi M, Hill JP, Meyer KA, Tsay C, Arnold CB, Smits AJ (2010) Turbulence measurements using a nanoscale thermal anemometry probe. J Fluid Mech 663:160–179

Chin C, Hutchins N, Ooi A, Marusic I (2011) Spatial resolution correction for hot-wire anemometry in wall turbulence. Exp Fluids 50:1443–1453

Chin CC, Hutchins N, Ooi ASH, Marusic I (2009) Use of direct numerical simulation (DNS) data to investigate spatial resolution issues in measurements of wall-bounded turbulence. Meas Sci Technol 20(11):115,401

Clauser F (1956) The turbulent boundary layer. Adv Appl Mech 4:1–51

DeGraaff DB, Eaton JK (2000) Reynolds-number scaling of the flat-plate turbulent boundary layer. J Fluid Mech 422:319–346

Hoyas S, Jiménez J (2006) Scaling of the velocity fluctuations in turbulent channels up to $Re_\tau = 2003$. Phys Fluids 18(1):011,702

Hultmark M, Bailey SCC, Smits AJ (2010) Scaling of near-wall turbulence in pipe flow. J Fluid Mech 649:103–113

Hultmark M, Ashok A, Smits A (2011) A new criterion for end-conduction effects in hot-wire anemometry. Meas Sci Technol 22.5:055,401

Hultmark M, Vallikivi M, Bailey SCC, Smits AJ (2012) Turbulent pipe flow at extreme reynolds numbers. Phys Rev Lett 108:094,501. doi:10.1103/PhysRevLett.108.094501

Hultmark M, Vallikivi M, Bailey S, Smits A (2013) Logarithmic scaling of turbulence in smooth- and rough-wall pipe flow. J Fluid Mech (in press):20

Hutchins N, Nickels TB, Marusic I, Chong MS (2009) Hot-wire spatial resolution issues in wall-bounded turbulence. J Fluid Mech 635(–1):103–136

Li J, McKeon B, Jiang W, Morrison J, Smits A (2004) The response of hot wires in high reynolds-number turbulent pipe flow. Meas Sci Technol 15:789–798

Ligrani PM, Bradshaw P (1987) Spatial resolution and measurement of turbulence in the viscous sublayer using subminiature hot-wire probes. Exp Fluids 5(6):407–417

Lozano-Durán A, Jiménez J (2014) Effect of the computational domain on direct simulations of turbulent channels up to $Re_\tau = 4200$. Phys Fluids 26:011,702

Marusic I, Monty J, Hutchins N, Smits A (2010) Spatial resolution and Reynolds number effects in wall-bounded turbulence. In: Proceedings of the 8th international ERCOFTAC symposium on engineering turbulence modelling and measurements (ETMM8)

Monkewitz P, Duncan R, Nagib H (2010) Correcting hot-wire measurements of stream-wise turbulence intensity in boundary layers. Phys Fluids 22:091,701

Monty JP (2005) Developments in smooth wall turbulent duct flows. PhD thesis, University of Melbourne

Monty JP, Stewart JA, Williams RC, Chong M (2007) Large-scale features in turbulent pipe and channel flows. J Fluid Mech 589:147–156

Ng HCH, Monty JP, N H, Chong MS, Marusic I (2011) Comparison of turbulent channel and pipe flows with varying Reynolds number. Exp Fluids 51(5):1261–1281

Örlü R, Alfredsson P (2013) Comment on the scaling of the near-wall streamwise variance peak in turbulent pipe flows. Exp Fluids 54:1431

Perry AE (1982) Hot-wire anemometry. Oxford University Press, Oxford

Philip J, Baidya R, Hutchins N, Monty J, Marusic I (2013a) Spatial averaging of streamwise and spanwise velocity measurements in wall-bounded turbulence using v- and x-probes. Meas Sci Technol 24:115,302

Philip J, Hutchins N, Monty J, Marusic I (2013b) Spatial averaging of velocity measurements in wall-bounded turbulence: single hot-wires. Meas Sci Technol 24(11):115,301

Pope SB (2000) Turbulent flows. Cambridge University Press, Cambridge

Schlatter P, Örlü R (2010) Assessment of direct numerical simulation data of turbulent boundary layers. J Fluid Mech 659:116–126

Segalini A, Örlü R, Schlatter P, Alfredsson P, Rüedi JD, Talamelli A (2011) A method to estimate turbulence intensity and transverse taylor microscale in turbulent flows from spatially averaged hot-wire data. Exp Fluids 51:693–700

Smits AJ, Monty JP, Hultmark M, Bailey SCC, Hutchins N, Marusic I (2011) Spatial resolution correction for wall-bounded turbulence measurements. J Fluid Mech 676:41–53

Talamelli A, Segalini A, Örlü R, Schlatter P, Alfredsson P (2013) Correcting hot-wire spatial resolution effects in third- and fourth-order velocity moments in wall-bounded turbulence. Exp Fluids 54:1496

Tavoularis S (2005) Measurement in fluid mechanics. Cambridge University Press, Cambridge

Townsend AA (1976) The structure of turbulent shear flow. Cambridge University Press, Cambridge

Vallikivi M, Hultmark M, Bailey SCC, Smits AJ (2011) Turbulence measurements in pipe flow using a nano-scale thermal anemometry probe. Exp Fluids 51:1521–1527

Wu X, Moin P (2008) A direct numerical simulation study on the mean velocity characteristics in turbulent pipe flow. J Fluid Mech 608:81–112

Yakhot V, Bailey SCC, Smits AJ (2010) Scaling of global properties of turbulence and skin friction in pipe and channel flows. J Fluid Mech 652:65–73

Zanoun ES, Durst F, H N (2003) Evaluating the law of the wall in two-dimensional fully developed turbulent channel flows. Phys Fluids 15:3079–3089